Random-Phase Approximation Calculation of the Scattering Function for Multicomponent Polymer Systems

Jin Kon Kim*

R&D Center, Petrochemicals & Polymers, Lucky Ltd., Science Town, P.O. Box 10, Daejeon, Korea 305-343

Kohtaro Kimishima and Takeji Hashimoto*

Department of Polymer Chemistry, Kyoto University, Kyoto 606, Japan

Received May 15, 1992; Revised Manuscript Received September 24, 1992

ABSTRACT: A method for calculating the structural factor, $\tilde{S}_{ij}(q)$, for multicomponent polymer systems is described using a random-phase approximation and incompressibility constraint. Also, for 4-component polymer systems, all $\tilde{S}_{ij}(q)$ are obtained in explicit forms. Among the many possible choices of 4-component polymer systems, we considered only two special cases: (i) a mixture of two block copolymers, (A-B)/(C-D), and (ii) a mixture of a block copolymer and two homopolymers, (A-B)/C/D, where the diblock copolymer C-D has a chemical structure different from the diblock copolymer A-B, and the two homopolymers, C and D, have chemical structures different from the constituent blocks of the diblock copolymer A-B. The spinodal points, where all $\tilde{S}_{ij}(q)$ become infinite, of microphase and macrophase transitions, respectively, for the two cases are discussed in detail.

I. Introduction

In recent years, block copolymers have been used to improve the compatibility of two immiscible homopolymers.[1] For example, polystyrene-*block*-polybutadiene (SB diblock) copolymer has been used to improve the compatibility between polystyrene (PS) and polyethylene (PE), thereby improving the mechanical properties of PS/PE blends. Similarly, polystyrene-*block*-poly(ethylene-*co*-butylene)-*block*-polystyrene (SEBS triblock) copolymer has been used to improve the impact strength of poly(phenylene ether)/polyamide blends.

Compatibilization of two immiscible homopolymers by addition of a diblock copolymer has recently been studied theoretically.[2-6] These studies considered primarily the concentration profile at the interface between the constituent components. From the point of view of preparing multicomponent blend systems, the construction of a phase diagram is the most desirable. At present, however, there is no theory available which will enable one to construct a phase diagram for 4-component polymer systems such as the (A-B)/C/D blend system, where homopolymers C and D have chemical structures that are different from the block copolymer A-B. The only theories available at present are the those of Hong and Noolandi[7] and Whitmore and Noolandi,[8] which enable one to construct a phase diagram for the (A-B)/C blend system (i.e., $m = 3$).

The structure factor $\tilde{S}_{ij}(q)$ has long been calculated using a random-phase approximation (RPA).[9,10] Since Leibler[11] first calculated $\tilde{S}_{ij}(q)$ for monodisperse diblock copolymers, other research groups[7,8,12-23] have extended the RPA method to calculate $\tilde{S}_{ij}(q)$ for (i) mixtures of a block copolymer and homopolymer and (ii) block copolymers having multiblocks[23] or star-shaped blocks.[17,21] Still others[12,24-28] included the polydispersity effect in the calculation of $\tilde{S}_{ij}(q)$, via RPA, for mixtures of a block copolymer and hompolymers. Specifically, Ijichi and Hashimoto[20] obtained explicit expressions for $\tilde{S}_{ij}(q)$ for 3-component polymer systems, and Vilgis et al.[15] and Benmouna and Vilgis[16] introduced three different methods (i.e., Ornstein-Zernike (OZ) formalism, RPA method, and Edwards-Hamiltonian methods) to the calculation of $\tilde{S}_{ij}(q)$ for multicomponent polymer systems. Here, "m-component" polymer system refers to a multicomponent system consisting of m different monomers. Therefore, the diblock copolymer consisting of components A and B can be regarded as a 2-component polymer system, and a mixture consisting of a diblock copolymer, (A-B), and two homopolymers, C and D, can be regarded as a 4-component polymer system.

In this paper, we shall first present a method to calculate $\tilde{S}_{ij}(q)$ explicitly for multicomponent (especially $m \geq 4$) polymer systems by extending the RPA method. And then, we shall apply the method to the following specific cases: (i) mixtures of two block copolymers, (A-B) and (C-D) and (ii) mixtures of a block copolymer (A-B) and two homopolymers C and D. Emphasis will be placed on discussing the stability limits for the microphase and macrophase separation, respectively, in the 4-component polymer systems.

II. Theory

Let us consider an m-component polymer system. In this situation, the scattering intensity $I(q)$ is given by

$$I(q) \sim \sum_{i,j=1}^{m} a_i a_j \tilde{S}_{ij}(q) \tag{1}$$

where a_i ($i = 1, 2, ... m$) corresponds to the scattering power of monomer i and $q = (4\pi/\lambda) \sin (\Theta/2)$, in which λ and Θ are the wavelength of the incident radiation and scattering angle in the medium, respectively. Applying the incompressibility constraint and symmetry property (i.e., $\tilde{S}_{ij}(q) = \tilde{S}_{ji}(q)$) to eq 1, we obtain

$$I(q) \sim \sum_{i,j}^{m-1} (a_i - a_m)(a_j - a_m)\tilde{S}_{ij}(q) \tag{2}$$

Note that the total number of independent components in $\tilde{S}_{ij}(q)$ for the *incompressible* m-component polymer system is $m(m - 1)/2$.

It should be mentioned that the incompressibility constraint must be used very carefully. Recently, some research groups[29-35] questioned the validity of the use of the incompressibility constraint in the RPA calculation. Since a free volume may exist in polymer blends in the molten state, it is reasonable to consider the finite compressibility. On the basis of the equation of state, Sanchez and Lacomb[36] included the free-volume term in the calculation of the phase diagram of polymer blends which exhibit the lower critical solution temperature (LCST). Benoit[30] has formulated the RPA expression for the compressible system. By use of the Edwards Hamiltonian, Freed and co-workers[31-35] obtained RPA expressions for the compressible blend and block copolymer melts. They[33] found that (i) the structure factor, $\tilde{S}_{AA}(q)$, for the block copolymer with finite compressibility does not become zero in the limit of $q \to 0$, while $\tilde{S}_{AA}(0)$ for the block copolymer with incompressibility is equal to zero and that (ii) significant differences between compressible and incompressible RPA structure factors arise in blends and block copolymers near the phase- or microphase-transition temperature. Very recently, Dudowicz and Freed[34,35] showed that the finite compressibility must be considered in order to explain experimental results obtained from small-angle neutron scattering (SANS) for the phase behaviors of a polystyrene/poly(vinyl methyl ether) blend.

Note that for the *compressible* m-component polymer system the total number of independent components in $\tilde{S}_{ij}(q)$ is $m(m+1)/2$. Also, the void volume fraction, ϕ_v, and additional interaction parameters between each component and the void volume (i.e., free volume), χ_{iv} ($i = 1 - m$), which are very difficult to measure experimentally, are needed to obtain $\tilde{S}_{ij}(q)$ for the compressible m-component polymer system.

Thus, even if we are well aware of the argument against the incompressibility assumption, we shall use this assumption for the reason that it allows us to perform relatively straightforward calculations for $\tilde{S}_{ij}(q)$ for an m-component polymer system.

Applying the RPA method to the m-component polymer system, one has[9-11]

$$\delta n_i(q) = -\beta \sum_{i=1}^{m} S_{ij}(q) U_j^{\text{eff}}(q) \tag{3a}$$

$$(i = 1, 2, \ldots, m)$$

$$U_j^{\text{eff}}(q) = U_j(q) + (1/\beta) \sum_{k \neq j}^{m} \chi_{jk} \delta n_k(q) + V\xi_j \tag{3b}$$

where $S_{ij}(q)$ is the ideal response function, i.e., the Fourier transform of the density–density correlations of monomers i and j for ideal Gaussian chains; $U_j(q)$ is the external potential exerted by adding the jth monomer; δn_i is the concentration fluctuation of monomer i; $\beta = 1/k_BT$ in which k_B is the Boltzmann constant and T is the absolute temperature; χ_{jk} is the Flory interaction parameter between monomers j and k; V is the potential required to assure incompressibility; and vector $\boldsymbol{\xi}$ having m components is given by $(1, 1, \ldots, 1, 1)^T$, in which superscript T denotes the transpose of the vector $\boldsymbol{\xi}$.

With the incompressibility constraint, $\sum_{i=1}^{m} \delta n_i = 0$, from eq 3 we obtain

$$V = \frac{\sum_{k=1}^{m-1} \delta n_k [1 + S_{mj}(q)(\chi_{jm} - \chi_{jk})] - \beta S_{mj}(q) U_j(q)}{\beta S_{mj}(q) \xi_j} \tag{4}$$

By combining eqs 3 and 4, we obtain the following expression for $\delta n_i(q)$:

$$\mathbf{A} \cdot \delta\mathbf{n}(q) = \beta \mathbf{B} \tag{5}$$

where $\mathbf{A}$ is an $(n-1) \times (n-1)$ matrix and given by

$$A_{ij}(q) = \sum_{p=1}^{m} [S_{ip}(q) - \upsilon_i(q) S_{mp}(q)][\chi_{pj} - \chi_{pm}] + \upsilon_i(q) + \delta_{ij} \tag{6}$$

and $\delta\mathbf{n}(q)$ and $\mathbf{B}$, having $(n-1)$ components, are given by

$$\delta\mathbf{n}(q) = [\delta n_1(q), \delta n_2(q), \ldots, \delta n_{m-1}(q)]^T \tag{7}$$

$$B_i(q) = \sum_{p=1}^{m} [S_{mp}(q) \upsilon_i(q) - S_{ip}(q)][U_p(q) - U_m(q)] \tag{8}$$

Note that $\upsilon_i(q)$ is given by

$$\upsilon_i(q) = t_i(q)/t_m(q) \tag{9a}$$

where

$$t_j(q) = \sum_{r=1}^{m} S_{jr}(q) \tag{9b}$$

And, $\delta n_i(q)$ appearing in eq 7 is also given by[9-11]

$$\delta n_i(q) = -\beta \sum_{j=1}^{m} \tilde{S}_{ij}(q) U_j(q) \tag{10}$$

Applying the incompressibility constraint and symmetry properties of $\tilde{S}_{ij}(q)$ to eq 10, we obtain

$$\delta n_i(q) = -\beta \sum_{k=1}^{m-1} \tilde{S}_{ik}(q)[U_k(q) - U_m(q)] \tag{11}$$

Since $\delta n_i(q)$ in eqs 5 and 11 must be the same, we have the structure factor $\tilde{S}_{ij}(q)$:

$$\tilde{S}_{ij}(q) = \sum_{k=1}^{m-1} \mathbf{A}_{ik}^{-1}(q)[S_{kj}(q) - \upsilon_k(q) S_{mj}(q)] \tag{12}$$

$$(i = 1, 2, \ldots m-1;\ j = 1, 2, \ldots m-1)$$

where $\mathbf{A}^{-1}$ is the inverse of matrix $\mathbf{A}$, whose components are defined by eq 6. From eq 12 the spinodal point of an m-component system can be obtained easily since every $\tilde{S}_{ij}(q)$ has the determinant of $A_{ij}(q)$ in the denominator. Note that if the determinant of $A_{ij}(q)$ is equal to zero, all $\tilde{S}_{ij}(q)$ become infinite.

At this juncture, let us compare eq 12 with the method introduced by Benoit and co-workers,[15,16] who obtained $\tilde{S}_{ij}(q)$ for multicomponent polymer systems as follows:

$$\tilde{\mathbf{S}}^{-1}(q) = \mathbf{S}_o^{-1}(q) + \mathbf{U}(q) \tag{13}$$

where $\mathbf{S}_o(q)$ and $\mathbf{U}(q)$ are the bare (or single-chain) structure matrix and the interaction (or excluded-volume) matrix, respectively. $\mathbf{U}(q)$ in eq 13 should not be confused with $U_j(q)$ in eq 3. Note that the matrices of $\tilde{\mathbf{S}}(q)$, $\mathbf{S}_o(q)$, and $\mathbf{U}(q)$ have $(m-1) \times (m-1)$ components.

In order to facilitate a comparison of eq 12 with eq 13, eq 12 can be rewritten with the aid of eq 6 in the following matrix form:

$$\tilde{\mathbf{S}}^{-1}(q) = [\mathbf{S}_o - \delta\mathbf{S}_o(q)]^{-1} + (\boldsymbol{\chi}_o - \delta\boldsymbol{\chi}_o) + [\mathbf{S}_o(q) - \delta\mathbf{S}_o(q)]^{-1} \cdot (\mathbf{X} + \mathbf{v}_o \boldsymbol{\xi}_o) \tag{14}$$

where all matrices are $(m-1) \times (m-1)$ matrices, given by

$$\mathbf{S}_o(q) = S_{ij}(q) \tag{15a}$$

$$(\delta \mathbf{S}_o(q))_{ij} = v_i(q)S_{mj}(q) \qquad (15b)$$

$$\chi_o = \chi_{ij} \qquad (15c)$$

$$(\delta \chi_o)_{ij} = \chi_{im} \qquad (15d)$$

$$(\mathbf{X})_{ij} = [S_{im}(q) - v_i(q)S_{mm}(q)]\chi_{mj} \qquad (15e)$$

$$\mathbf{v}_o(q) = (v_1(q), v_2(q) \ldots, v_{m-1}(q))^{\mathrm{T}} \qquad (15f)$$

$$\boldsymbol{\xi}_o = (1, 1 \ldots, 1)^{\mathrm{T}} \quad (m - 1 \text{ vector}) \qquad (15g)$$

In order for eq 14 to be equivalent to eq 13, the following conditions must be satisfied:

$$\delta \mathbf{S}_o = 0 \qquad (16a)$$

$$\mathbf{U}(q) = (\chi_o - \delta\chi_o) + [\mathbf{S}_o(q)]^{-1} \cdot (\mathbf{X} + \mathbf{v}_o \boldsymbol{\xi}_o) \qquad (16b)$$

Notice that when there is at least one homopolymer (or solvent) in the mixture and if the homopolymer (or solvent) is taken as the mth component, all $S_{mj}(q)$ ($j = 1, 2, \ldots, m - 1$) are equal to zero. In such a situation, eq 16a is automatically satisfied since $\delta \mathbf{S}_o(q)$ becomes a zero matrix (see eq 15b). For mixtures of a block copolymer (A–B) and homopolymer C (i.e., 3-component system), eq 16b reduces to eqs 19a and b in ref 16 (see Appendix I). However, when there is no homopolymer (or solvent) present in the mixture, $\delta \mathbf{S}_o(q)$ is not a zero matrix since at least one component in $S_{mj}(q)$ is not equal to zero, and $\mathbf{U}(q)$ given in eqs 19a and b in ref 16 cannot be used. Therefore, we can say that eq 14 (or eq 12) is more general than eq 1 in refs 15 and 16. Notice further that, for the 3-component polymer systems, calculations of $\tilde{S}_{ij}(q)$ from eq 13 can easily be done. For 4-component polymer systems, however, $\tilde{S}_{ij}(q)$ from eq 13 can be obtained only by a trial-and-error method even when $\mathbf{U}(q)$ is known (see Appendix I). On the other hand, the calculation of $\tilde{S}_{ij}(q)$, via eq 12, for multicomponent systems is straightforward since the inverse of the matrix $A_{ij}(q)$ can easily be obtained numerically without using a trial-and-error method.

Although $\tilde{S}_{ij}(q)$ and the determinant of $A_{ij}(q)$ can easily be calculated numerically, one may be tempted to express $\tilde{S}_{ij}(q)$ in an explicit form. Since the structure factors $\tilde{S}_{ij}(q)$ in the explicit form for the 3-component systems were already obtained by one of us,[20,37] we shall consider the 4-component polymer systems (i.e., $m = 4$), which can represent mixtures of two block copolymers, (A–B) and (C–D), or mixtures of a block copolymer (A–B) and two homopolymers C and D. Notice that the chemical structures of C and D are different from those of A and B.

After long mathematical manipulations, for $m = 4$ we can express the determinant ($\|D\|$) of $A_{ij}(q)$ as

$$\|D\| = [S_4(q)/t_4(q)]/F(q) \qquad (17)$$

where $S_4(q)$ is the sum of $S_{ij}(q)$:

$$S_4(q) = \sum_{i=1}^{4} t_i(q) = \sum_{i,j=1}^{4} S_{ij}(q) \qquad (18)$$

and $F(q)$ is given by

$$F(q) = 1 + \sum_{i,j}^{4} \bar{S}_{ij}(q)\chi_{ij} + \sum_{\substack{i,j\\k,\ell}}^{4} D_{2,ijk\ell}(q)\chi_{ij}\chi_{k\ell} + 2[W_4(q)/S_4(q)]\chi^*{}_{\mathrm{D}} \qquad (19)$$

where $W_4(q)$ is the determinant of $S_{ij}(q)$

$$W_4(q) = \|S_{ij}(q)\| \qquad (20a)$$

and

$$\bar{S}_{ij}(q) = S_{ij}(q) - t_i(q)t_j(q)/S_4(q) \qquad (20b)$$

$$D_{2,ijk\ell}(q) = ({}^1/_4)\{2[S_{ij}(q)\bar{S}_{k\ell}(q) + S_{k\ell}(q)\bar{S}_{ij}(q)] - [S_{ik}(q)\bar{S}_{j\ell}(q) + S_{j\ell}(q)\bar{S}_{ik}(q) + S_{i\ell}(q)\bar{S}_{jk}(q) + S_{jk}(q)\bar{S}_{i\ell}(q)] + S_{ik}(q)S_{j\ell}(q) + S_{i\ell}(q)S_{jk}(q) - 2S_{ij}(q)S_{k\ell}(q)\} \qquad (20c)$$

$$\chi^*{}_{\mathrm{D}} = \chi_{12}\chi_{13}\chi_{23} + \chi_{12}\chi_{14}\chi_{24} + \chi_{23}\chi_{24}\chi_{34} + \chi_{13}\chi_{14}\chi_{34} - [(\chi_{12} + \chi_{34})(\chi_{13}\chi_{24} + \chi_{14}\chi_{23} - \chi_{12}\chi_{34}) + (\chi_{13} + \chi_{24})(\chi_{12}\chi_{34} + \chi_{14}\chi_{23} - \chi_{13}\chi_{24}) + (\chi_{14} + \chi_{23})(\chi_{12}\chi_{34} + \chi_{13}\chi_{24} - \chi_{14}\chi_{23})] \qquad (20d)$$

Note that for 3-component systems, eq 19 can be reduced to eq 21 in ref 20, since $W_4(q) = 0$, $S_4(q) = S_3(q)$, $D_{2,1212}(q) = D_{2,1313}(q) = D_{2,2323}(q) = -({}^1/_4)W_3(q)/S_3(q)$, and $D_{2,1213}(q) = D_{2,1223}(q) = D_{2,1323}(q) = ({}^1/_4)W_3(q)/S_3(q)$. For mixtures of block copolymer (A–B) and homopolymer C, eq 19 becomes identical to eq 2.31 in ref 8 (see Appendix II) for predicting the spinodal point.

Finally, by substituting eqs 6 and 17 into eq 12, for $m = 4$ we obtain the structure factors $\tilde{S}_{\alpha\beta}(q)$:

$$\tilde{S}_{\alpha\beta}(q) = \{\bar{S}_{\alpha\beta}(q) + 2\sum_{k,\ell}^{4} D_{2,\alpha\beta k\ell}(q)\chi_{k\ell} + [W_4(q)/S_4(q)]\chi^*{}_{\alpha\beta,2}\}/F(q) \qquad (21)$$

$$(\alpha = 1, 2, 3;\ \beta = 1, 2, 3)$$

where

$$\chi^*{}_{\alpha\alpha,2} = 2(\chi_{\gamma\delta}\chi_{\gamma\epsilon} + \chi_{\delta\epsilon}\chi_{\gamma\delta} + \chi_{\gamma\epsilon}\chi_{\delta\epsilon}) - (\chi_{\gamma\delta}{}^2 + \chi_{\delta\epsilon}{}^2 + \chi_{\gamma\epsilon}{}^2) \qquad (22a)$$

$$(\gamma \neq \delta \neq \epsilon \neq \alpha \text{ and } \gamma < \delta < \epsilon)$$

$$\chi^*{}_{\alpha\beta,2} = 2(\chi_{\alpha\beta}\chi_{\gamma\delta} + \chi_{\alpha\gamma}\chi_{\beta\gamma} + \chi_{\alpha\delta}\chi_{\beta\delta}) - \chi_{\gamma\delta}(\chi_{\alpha\gamma} + \chi_{\alpha\delta} + \chi_{\beta\gamma} + \chi_{\beta\delta}) - \chi_{\alpha\gamma}\chi_{\beta\delta} - \chi_{\alpha\delta}\chi_{\beta\gamma} + \chi_{\delta\gamma}{}^2 \qquad (22b)$$

$$(\gamma \neq \delta \neq \alpha \neq \beta \text{ and } \gamma < \delta)$$

The indexes α, β, γ, δ, and ϵ appearing in eqs 21 and 22 are not dummy variables, so the summation of these indexes must not be taken. From eq 21 $\tilde{S}_{11}(q)$, for example, is given by

$$\tilde{S}_{11}(q) = \{\bar{S}_{11}(q) + 2\sum_{k,\ell}^{4} D_{2,11k\ell}(q)\chi_{k\ell} + [W_4(q)/S_4(q)]\chi^*{}_{11,2}\}/F(q) \qquad (23)$$

where

$$\chi^*{}_{11,2} = 2(\chi_{23}\chi_{24} + \chi_{23}\chi_{34} + \chi_{24}\chi_{34}) - (\chi_{23}{}^2 + \chi_{24}{}^2 + \chi_{34}{}^2) \qquad (23a)$$

III. Spinodal Decomposition for 4-Component Polymer System

(a) Stability of $F(q)$. For 4-component systems, the scattering intensity $I(q)$ is given by eq 2:

$$I(q) \sim \sum_{i,j=1}^{3} (a_i - a_4)\,(a_j - a_4)\tilde{S}_{ij}(q) \qquad (24)$$

It can be seen from eq 24 that $I(q)$ cannot easily be determined quantitatively, even if all $\tilde{S}_{ij}(q)$ are known, in the situation where accurate information for all a_i is not available. Therefore, we consider only the stability limit, where $I(q)$ becomes infinite at $q = q^*$:

$$I(q^*) \rightarrow \infty \tag{25}$$

Since all components of $\tilde{S}_{ij}(q)$ have the common denominator $F(q)$ (see eq 21), $I(q)$ becomes infinite when $F(q)$ is equal to zero.

In order to calculate $F(q)$ for 4-component systems, we need six different Flory interaction parameters, χ_{12}, χ_{13}, χ_{14}, χ_{23}, χ_{24}, and χ_{34}, and four different values of degree of polymerization, N_1, N_2, N_3, and N_4. For given values of N_i (i = 1–4), $\{(\chi_s)_{ij}\}$, which makes $F(q^*)$ equal to zero, can exist. Note that q^* can be obtained from the value of q_m where $F(q_m{=}q^*)$ becomes zero (or $I(q_m{=}q^*)$ diverges to infinity) at $(\chi_s)_{ij}$. q_m is the value of q which makes $F(q)$ a minimum at given χ_{ij}, and q_m can change with χ_{ij} for 4-component polymer systems. For $q^* = 0$, $\{(\chi_s)_{ij}\}$ describes the spinodal or the limit of thermodynamic stability for the *macrophase* transition (or separation), whereas for $q^* \neq 0$, $\{(\chi_s)_{ij}\}$ describes the spinodal point for the *microphase* transition (or separation).

Since a criterion for the stability limit (or relationships between χ_{ij}) for 4-component systems is very difficult to obtain analytically, let us consider a *special* case where all N_i and the ratio χ_{ij}/χ_{12}, except for χ_{12}, are fixed. In such a situation, the spinodal transition in terms of $(\chi N_1)_s$ can be obtained from

$$F[q^*,(\chi N_1)_s] = 0 \tag{26}$$

where χ is χ_{12} and N_1 is the degree of polymerization of component 1. In order to check whether or not eq 26 is indeed satisfied, we rearrange eq 19 as

$$F[q,(\chi N_1)] = 1 + a_o(q)(\chi N_1) + b_o(q)(\chi N_1)^2 + c_o(q)(\chi N_1)^3 \tag{27}$$

where

$$a_o(q) = \sum_{i,j}^{4} [\tilde{S}_{ij}(q)] R_{ij}/N_1 \tag{28a}$$

$$b_o(q) = \sum_{\substack{i,j\\k,\ell}}^{4} [D_{2,ijk\ell}(q)] R_{ij} R_{k\ell}/N_1^2 \tag{28b}$$

$$c_o(q) = 2[W_4(q)/S_4(q)](\chi^*_D/\chi^3)/(N_1)^3 \tag{28c}$$

in which

$$R_{ij} = \chi_{ij}/\chi \tag{29a}$$

$$\chi = \chi_{12} \tag{29b}$$

Note that since every $S_{ij}(q)$ in $D_{2,ijk\ell}(q)$ and $W_4(q)$ contains N_k (k = 1–4), $a_o(q)$, $b_o(q)$, and $c_o(q)$ in eq 28 have R_{ij} and N_k implicitly.

Let us now consider several specific cases:

(i) $c_o(q) = 0$. This case can be obtained from the following relationships for χ_{ij}:

$$R_{34} = 1 \tag{30a}$$

$$R_{14} = R_{23} = \alpha \tag{30b}$$

$$R_{13} = R_{24} = 1 - \alpha \tag{30c}$$

where $0 \leq \alpha \leq 1$, since eq 30 gives $\chi^*_D = 0$. Note that when α is equal to unity, the 4-component system under consideration represents a mixture of two block copolymers, $(A\text{–}B)_1$ and $(A\text{–}B)_2$, having the same structure. Therefore, in this situation, the following relationship must be satisfied in order to obtain a definite value for $(\chi N_1)_s$:

$$[a_o(q^*)]^2 \geq 4b_o(q^*) \tag{31}$$

It should be mentioned that eqs 30a–c can be applied to a special 4-component system. Since there are six independent χ_{ij} (i.e., χ_{12}, χ_{13}, χ_{14}, χ_{23}, χ_{24}, and χ_{34}) in eq 27, five dependent equations given by eqs 30a–c leave only one unknown χ (i.e., χ_{12}). Therefore, eq 27 can be solved if χ_{12} is known. But, since χ_{ij} is usually expressed by the solubility parameters of the monomers i and j (δ_i and δ_j), six χ_{ij} are expressed by only four solubility parameters, δ_i (i = 1–4). For example, χ_{12} is given by

$$\chi_{12} \sim (\delta_1 - \delta_2)^2 \tag{32}$$

In this situation, α in eqs 30b and c must be equal to 1 or 0 (i.e., a mixture of $(A\text{–}B)_1$ and $(A\text{–}B)_2$) when the relationships for χ_{ij} are given by eqs 30a–c.

But, due to specific interactions such as the hydrogen-bonding force between the monomers i and j, the values of χ_{ij} cannot be determined by the solubility parameters alone. Therefore, we will continue to use the very special relationships for χ_{ij} given by eqs 30a–c for the 4-component systems.

(ii) $c_o(q) \neq 0$. In this case, one can easily know that at least one value of $(\chi N_1)_s$, which may be either positive or negative, exists due to the characteristics of the cubic function $F(q)$ with respect to χN_1.

(b) Mixture of Two Block Copolymers (A–B) and (C–D). For mixtures of block copolymer (A–B) and block copolymer (C–D) $S_{ij}(q)$ are given by

$$S_{11}(q) = \phi_1 N_1 g(f_1,N_1) \tag{33a}$$

$$S_{22}(q) = \phi_1 N_1 g(1-f_1,N_1) \tag{33b}$$

$$S_{33}(q) = (1 - \phi_1) N_3 g(f_3,N_3) \tag{33c}$$

$$S_{44}(q) = (1 - \phi_1) N_3 g(1-f_3,N_3) \tag{33d}$$

$$S_{12}(q) = (^1/_2)\phi_1 N_1 [g(1,N_1) - g(f_1,N_1) - g(1-f_1,N_1)] \tag{33e}$$

$$S_{34}(q) = (^1/_2)(1 - \phi_1) N_3 [g(1,N_3) - g(f_3,N_3) - g(1-f_3,N_3)] \tag{33f}$$

$$S_{13}(q) = S_{14}(q) = S_{23}(q) = S_{24}(q) = 0 \tag{33g}$$

where ϕ_1 and $1 - \phi_1$ are the volume fractions of block copolymers (A–B) and (C–D), respectively, f_1 is the volume fraction of component A in block copolymer (A–B) and f_3 is the volume fraction of C in block copolymer (C–D), and $f_1 N_1$, $(1 - f_1)N_1$, $f_3 N_3$, and $(1 - f_3)N_3$ are degrees of polymerization (or number of statistical segments) for A–D chain segments, respectively. Also $g(f_i,N_i)$ is given by

$$g(f_i,N_i) = 2[f_i x_i + \exp(-f_i x_i) - 1]/x_i^2 \tag{34a}$$

where

$$x_i = N_i q^2 a^2/6 \tag{34b}$$

Note that the statistical segment length, a, in eq 34b is assumed to be the same for all polymers A–D. For illustration purposes, let us consider a special case, where all R_{ij} are given by eq 30. Note that when eq 30 is used, $F(q)$ in eq 27 becomes a quadratic function with respect to (χN_1), since χ^*_D in $c_o(q)$ is equal to zero (see eq 20d).

For $f_1 = 1 - f_3 = 0.2$, $N_3 = (^1/_4)N_1$, and $\alpha = 0.2$, plots of $F(q)$ versus qR_{g1} for various values of χN_1 at $\phi_1 = 0.4$ and

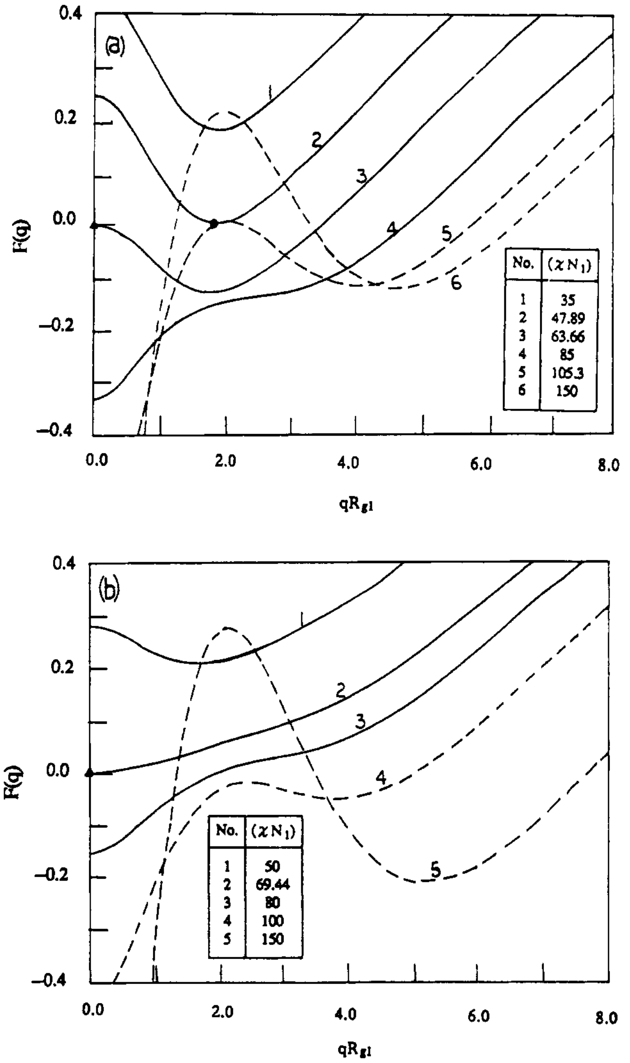

Figure 1. Plots of $F(q)$ versus qR_{g1} for $f_1 = 1 - f_3 = 0.2$, $N_3/N_1 = 0.25$, and $\alpha = 0.2$ for various χN_1 at different ϕ_1: (a) $\phi_1 = 0.4$; (b) $\phi_1 = 0.2$. Circle and triangle represent microphase and macrophase separations, respectively.

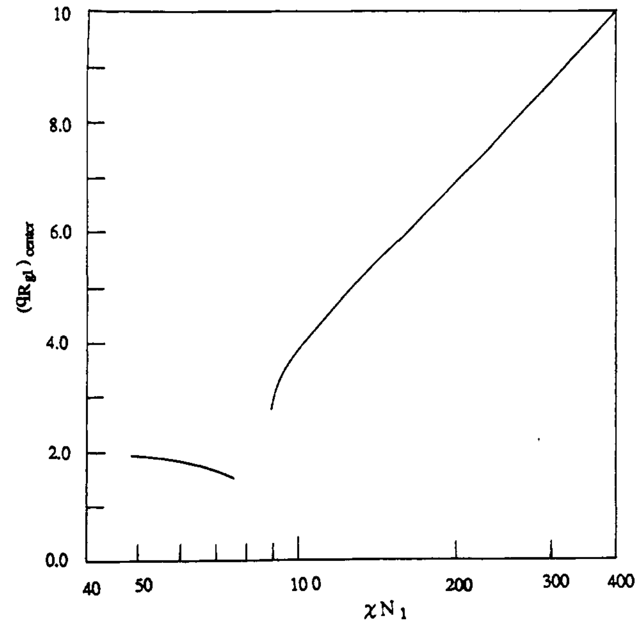

Figure 2. Plots of $(qR_{g1})_{\text{center}}$ versus χN_1 for $f_1 = 1 - f_3 = 0.2$, $N_3/N_1 = 0.25$, and $\alpha = 0.2$ at $\phi_1 = 0.4$.

0.2 are given in panels a and b, respectively, of Figure 1. Note that R_{g1} is the radius of gyration of the block copolymer (A–B). We have chosen two values of ϕ_1 (i.e., 0.4 and 0.2), since at $\phi_1 = 0.4$ the spinodal for the microphase transition, $(\chi N_1)_{\text{s,micro}}$, occurs more easily than that for the macrophase transition, $(\chi N_1)_{\text{s,macro}}$ (i.e., $(\chi N_1)_{\text{s,micro}} < (\chi N_1)_{\text{s,macro}}$), while at $\phi_1 = 0.2$ $(\chi N_1)_{\text{s,macro}}$ is less than $(\chi N_1)_{\text{s,micro}}$, which will be elaborated on below.

The following observations are worth noting in Figure 1a: (i) for $\chi N_1 < 47.9$, the system does *not* become *unstable* (i.e., it remains in a stable or metastable state) for both microphase and macrophase separations, since $F(q)$ is larger than 0 for all values of qR_{g1}; (ii) for $\chi N_1 = (\chi N_1)^{(-)} = 47.9$, $F(q^*)$ becomes zero at $(qR_{g1})^* = 1.86$, which corresponds to the spinodal for microphase separation, and the q mode at $(qR_{g1})^* = 1.86$ becomes unstable. Note that there exist two values of χN_1, $(\chi N_1)^{(-)}$, and $(\chi N_1)^{(+)}$ where $(\chi N_1)^{(-)} < (\chi N_1)^{(+)}$, from the solution of $F(q^*) = 0$ at $(qR_{g1})^*$, because $F(q)$ in eq 27 becomes a quadratic function with respect to χN_1 when eq 30 is used; (iii) for $\chi N_1 = (\chi N_1)_{\text{s,macro}} = 63.6$, $F(q{=}0)$ becomes zero, which corresponds to a spinodal for the macrophase transition since the mode with $q = 0$ becomes unstable; (iv) for $\chi N_1 = (\chi N_1)^{(+)} = 105.3$, $F(q)$ becomes zero again at $(qR_{g1})^* = 1.86$, but it does not have a minimum at $(qR_{g1})^*$; (v) for $\chi N_1 > (\chi N_1)^{(+)}$ (e.g., $\chi N_1 = 150$), the q mode with $(qR_{g1})^* = 1.86$ becomes stable, while the q modes satisfying $0 \leq qR_{g1} \leq 1.24$ and $3.32 \leq qR_{g1} \leq 6.48$ become unstable; and (vi) $(qR_{g1})_{\text{center}}$, which is the minimum point in the second unstable region appearing in curves 5 and 6, increases with increasing χN_1. It should be noted from curves 2 and 5 that only $(\chi N_1)^{(-)}$ becomes $(\chi N_1)_{\text{s,micro}}$, because for $(\chi N_1)^{(+)}$ $F(q)$ does not exhibit a minimum at $(qR_{g1})^*$ although $F(q^*)$ is equal to zero.

Also, the following observations are worth noting in Figure 1b: (i) for $\chi N_1 < 69.4$, the system does *not* become *unstable* (i.e., it remains in a stable or metastable state) for the macrophase separation, but the minimum in $F(q)$ occurs at $q = q_m \neq 0$; and (ii) for $\chi N_1 = (\chi N_1)_{\text{s,macro}} = 69.4$, $F(q^*{=}0)$ becomes zero, which corresponds to the spinodal for the macrophase transition where the q mode at $q = 0$ becomes unstable. It is of interest to note that the q modes around $qR_{g1} = 2$, which are unstable for small χN_1 (e.g., $\chi N \approx 100$), become stable with further increased values of χN_1 (e.g., $\chi N_1 \approx 150$), which is a trend similar to that shown in Figure 1a.

It is surprising to note in Figure 1 that, for larger values of χN_1 (e.g., curves 5 and 6 in (a) and curve 5 in (b)), there exist two unstable regions.[38] Note that $(qR_{g1})_{\text{center}}$ shifts continuously from $(qR_{g1})^*$ toward a larger value of q with increasing χN_1 (compare curve 5 with curve 6 in Figure 1a and compare curve 4 with curve 5 in Figure 1b). Therefore, we conclude that the unstable region on the left side is related only to macrophase separation, while the unstable region on the right side is related to microphase separation with the q mode of $(qR_{g1})_{\text{center}}$. To illustrate the point, plots of $(qR_{g1})_{\text{center}}$ versus χN_1 are given in Figure 2, from which we can observe that $(qR_{g1})_{\text{center}}$ changes little for $47.9 < \chi N_1 < 75$, but it increases significantly for $\chi N_1 > 90$. For $76 < \chi N_1 < 88$, $(qR_{g1})_{\text{center}}$ does not exist (see curve 4 in Figure 1a).

It should be mentioned that the values of $(qR_{g1})^*$ in Figure 1 were obtained from $(qR_{g1})_m$, where $F[(qR_{g1})_m]$ is equal to zero at a given $(\chi N_1)_s$. Note that for the (A–B)/(C–D) mixture, $(qR_{g1})_m$, which makes $F(q)$ a minimum at given χN_1, can vary with χN_1. This is quite different from the mixtures of two block copolymers having the same chemical structure, $(\text{A–B})_1/(\text{A–B})_2$, where $(qR_{g1})_m$ is the same as $(qR_{g1})^*$ regardless of the value of χN_1. To illustrate the point, let us consider the $(\text{A–B})_1/(\text{A–B})_2$ mixture (i.e., $\alpha = 1$), and plots of $F(q)$ versus qR_{g1} for

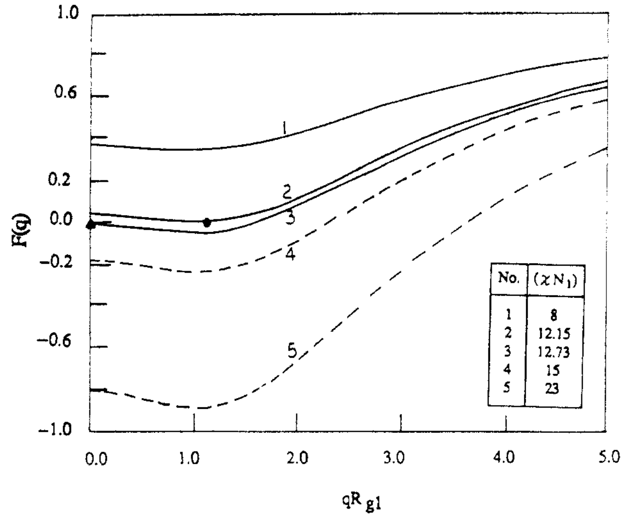

Figure 3. Plots of $F(q)$ versus qR_{g1} for $f_1 = 1 - f_3 = 0.2$, $N_3/N_1 = 0.25$, $\phi_1 = 0.4$, and $\alpha = 1$ for various χN_1. Circle and triangle represent microphase and macrophase separations, respectively.

various values of χN_1 at $\phi_1 = 0.4$ are given in Figure 3. It can be seen in Figure 3 that (i) for $\chi N_1 = (\chi N_1)_{s,\mathrm{micro}} = 12.15$, $F(q)$ becomes zero at $(qR_{g1})^* = 1.03$, and (ii) for $\chi N_1 > 12.15$, $F(q^*)$ becomes negative (i.e., unstable at q^*) and $(qR_{g1})_m$, which makes $F(q)$ a minimum, remains equal to $(qR_{g1})^*$ regardless of the value of χN_1. It should be mentioned that each curve in Figure 3 cannot be superimposed onto one another by a vertical shift. Note that for the $(A-B)_1/(A-B)_2$ mixture, $F(q)$ in eq 19 becomes

$$F(q) = [S(q)/W(q) - 2\chi][W(q)/S(q)] \qquad (35)$$

where

$$S(q) = S_{11}(q) + 2S_{12}(q) + S_{22}(q) + S_{33}(q) + 2S_{34}(q) + S_{44}(q) \qquad (36a)$$

$$W(q) = [S_{11}(q) + S_{33}(q)][S_{22}(q) + S_{44}(q)] - [S_{12}(q) + S_{34}(q)]^2 \qquad (36b)$$

But, according to ref 18, $f(q)$ is usually defined by

$$f(q) = S(q)/W(q) - 2\chi \qquad (37)$$

showing that the dependence of $f(q)$ on q does not vary with χ (or χN_1). Thus, $f(q)$ for various values of χ (or χN_1) can be superimposed onto one another by a vertical shift. However, according to eq 35, the dependence of $F(q)$ on q varies with χ and $F(q)$ for various χ (or χN_1) cannot be superimposed onto one another by a vertical shift, as shown in Figure 3.

Based on Figures 1 and 3, plots of $(\chi N_1)_s$ versus ϕ_1 for various values of α ($0 \leq \alpha \leq 1$) are given in Figure 4a–f. Note that the case of $\alpha = 1$, given in Figure 4a, corresponds to the $(A-B)_1/(A-B)_2$ mixture with $f_1 = 0.2$ and $f_3 = 0.8$, and the case of $\alpha = 0$, given in Figure 4f, corresponds to the $(A-B)_1/(A-B)_2$ mixture with $f_1 = f_3 = 0.2$ and $N_3/N_1 = {}^1/_4$, where f_3 is the volume fraction of A and N_3 is the total degree of polymerization in the block copolymer $(A-B)_2$.

The following observations are worth noting in Figure 4a–f: (i) with decreasing α, the stability for macrophase separation increases gradually, and the stability for microphase separation increases rapidly for $\phi_1 \geq 0.2$. Here, increased stability means a decrease in the transition temperature for the systems where χ decreases with increasing temperature or increasing $(\chi N_1)_s$; (ii) for $\alpha = 0$, the spinodal curve for the macrophase transition no longer exists; (iii) for $\alpha > 0.166$, in the region of $\phi_{1,\mathrm{CL}} \leq \phi_1 \leq \phi_{1,\mathrm{CR}}$, only the spinodal curves for macrophase transition exist; and (iv) for $\alpha = 0.166$, $\phi_{1,\mathrm{CL}}$ and $\phi_{1,\mathrm{CR}}$ have the same value (0.2). Note that $\phi_{1,\mathrm{CL}}$ (and $\phi_{1,\mathrm{CR}}$) is the volume fraction of the block copolymer (A–B) in the mixture below (and above) which the spinodal point for the microphase transition occurs more easily than that for the macrophase transition (i.e., $(\chi N_1)_{s,\mathrm{micro}} < (\chi N_1)_{s,\mathrm{macro}}$).

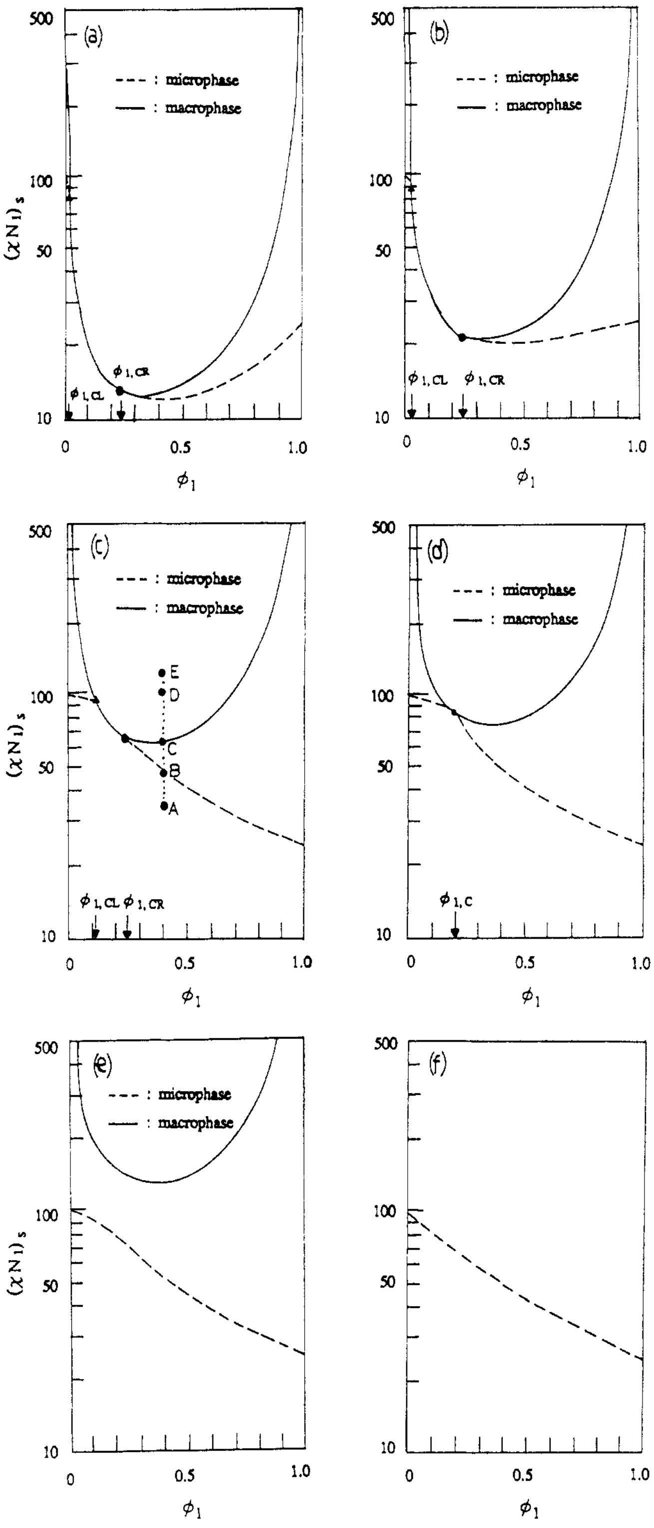

Figure 4. Spinodal curves for $f_1 = 1 - f_3 = 0.2$, and $N_3/N_1 = 0.25$ for various values of α: (a) 1.0; (b) 0.6; (c) 0.2; (d) 0.166; (e) 0.1; (f) 0.0.

The spinodal curves for the macrophase transition shown in Figure 4a–e were obtained by finding the values of $(\chi N_1)_{s,\mathrm{macro}}$ satisfying the following expressions:

$$F(q^*{=}0) = 0 \quad \text{for } \phi_{1,\mathrm{CL}} \leq \phi_1 \leq \phi_{1,\mathrm{CR}} \qquad (38a)$$

$$F(q=0) = 0 \quad \text{for } 0 < \phi_1 < \phi_{1,\mathrm{CL}} \text{ or } \phi_{1,\mathrm{CR}} < \phi_1 < 1 \tag{38b}$$

By substituting eqs 19, 20, 33, and 34 into eq 38, we obtain

$$1/[N_1\phi_1] + 1/[N_3(1-\phi_1)] = 2(\chi_{\mathrm{eff}})_{\mathrm{s}} \tag{39}$$

where

$$\chi_{\mathrm{eff}} = f_1f_3\chi_{13} + f_1(1-f_3)\chi_{14} + (1-f_1)f_3\chi_{23} + (1-f_1)(1-f_3)\chi_{24} - f_1(1-f_1)\chi_{12} - f_3(1-f_3)\chi_{34} \tag{40}$$

and $(\chi_{\mathrm{eff}})_{\mathrm{s}}$ is the effective Flory interaction parameter between the block copolymer (A–B) and the block copolymer (C–D) at the spinodal point. Note that, for the situations under consideration, $W_4(q=0)$ and all terms of $D_{2,ijk\ell}(q=0)$ in $F(q)$ (see eq 27) are equal to zero (or, $b_0(q=0) = c_0(q=0) = 0$). Thus $F(q)$ becomes a linear function of χN_1, and only one value of $(\chi N_1)_{\mathrm{s,macro}}$ exists. It should be mentioned that eqs 39 and 40 were derived previously by others,[18,39–41] who investigated the miscibility or stability limits for a mixture of two random copolymers, (A–B) and (C–D), based on the mean-field theory. Note that the mean-field spinodal point for the *macrophase* separation in a mixture of two block copolymers is the same as that in a mixture of two random copolymers and can easily be obtained from the Flory–Huggins theory with proper modification of the free energy.

It should be pointed out that in Figure 4 spinodal curves occurring for $\phi_{1,\mathrm{CR}} < \phi_1 < 1$ have a physical meaning different from those for $\phi_{1,\mathrm{CL}} \leq \phi_1 \leq \phi_{1,\mathrm{CR}}$. For example, point C in Figure 4c has physical meaning only in the case when the mixture is quenched from a single phase (e.g., point A in Figure 4c) to a state above point C. When the mixture is first quenched from a single phase to a state between point B and point C, point C cannot predict the spinodal from the state between point B and point C to a state above point C. In this sense, point C is not a spinodal for the macrophase transition in the *conventional* sense. In other words, at point C in Figure 4c, $F(q)$ is not a minimum at $q = 0$ although $F(q=0)$ is equal to zero, as shown in curve 3 in Figure 1a. The spinodal for macrophase separation in the *conventional* sense corresponds to the system where $F(q)$ is a minimum at $q = q^* = 0$ and $F(q^*=0) = 0$, as shown in curve 2 in Figure 1b. Note that the values of χN_1 at points A–E in Figure 4c were used to obtain curves 1–3, 5, and 6 in Figure 1a, respectively.

The observations made above in reference to Figure 4a–e (i.e., the stability for macrophase separation is enhanced with decreasing α) can be explained using eqs 30 and 40:

$$\frac{(\chi_{\mathrm{eff}})_\alpha}{(\chi_{\mathrm{eff}})_{\alpha=1}} = \frac{(f_1+f_3-1)^2 - \alpha(2f_1-1)(2f_3-1)}{(f_1+f_3-1)^2 - (2f_1-1)(2f_3-1)} \tag{41}$$

When $f_1 + f_3 = 1$ (except for $f_1 = f_3 = 0.5$), eq 41 reduces to

$$(\chi_{\mathrm{eff}})_\alpha/(\chi_{\mathrm{eff}})_{\alpha=1} = \alpha \tag{42}$$

For $0 < \alpha \leq 1$, the value of $(\chi_{\mathrm{eff}})_\alpha$ becomes smaller with decreasing α, which explains the enhanced stability for macrophase separation shown in Figure 4a–e. But eq 41 (or eq 42) cannot be used to predict the spinodal curves for *microphase* separation given in Figure 4a–f. Note from eq 39 that macrophase separation no longer exists when $(\chi_{\mathrm{eff}})_\alpha$ is equal to 0, which is the case for $\alpha = 0$, given in Figure 4f.

Plots of $(qR_{g1})^*$ versus ϕ_1 for various values of α are given in Figure 5. Note in Figure 5 that (i) for the mixtures having α greater than 0.166, with increasing ϕ_1, $(qR_{g1})^*$ decreases sharply in the region of $\phi_1 < \phi_{1,\mathrm{CL}}$, is zero for $\phi_{1,\mathrm{CL}} \leq \phi_1 \leq \phi_{1,\mathrm{CR}}$, and increases in the regime of $\phi_1 > \phi_{1,\mathrm{CR}}$; (ii) for the mixtures having α less than 0.166, $(qR_{g1})^*$ decreases gradually with increasing ϕ_1; and (iii) for the mixtures having α equal to 0.166, $(qR_{g1})^*$ for macrophase separation occurs at only one point, $\phi_1 = 0.2$.

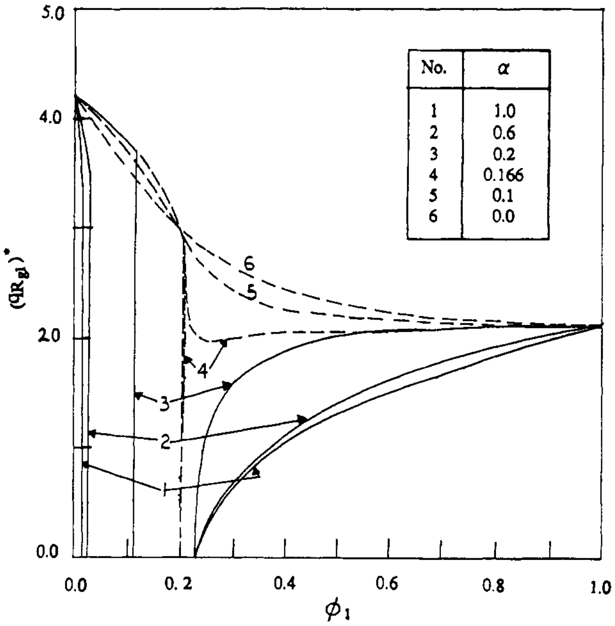

Figure 5. Plots of $(qR_{g1})^*$ versus ϕ_1 for $f_1 = 1 - f_3 = 0.2$, and $N_3/N_1 = 0.25$ for various values of α.

For $f_1 = 1 - f_3 = 0.5$, $N_3 = (^1/_4)N_1$, and $\alpha = 0.5$, plots of $F(q)$ versus qR_{g1} for various values of χN_1 are given in Figure 6a for $\phi_1 = 0.2$, Figure 6b for $\phi_1 = 0.1$, and Figure 6c for $\phi_1 = 0.35$. Note that this system does not have instability for macrophase separation, as is obvious from eqs 30 and 40 (i.e., $\chi_{\mathrm{eff}} = 0$ for all α). It can be seen from Figure 6a that (i) for $\chi N_1 < (\chi N_1)_{\mathrm{s,micro}} = 52.5$, the mixture does *not* become *unstable* (i.e., it remains in a stable or metastable state) for microphase transition; (ii) for $\chi N_1 = 52.5$, the mixture becomes unstable at two different modes, $(qR_{g1})^{*(1)} = 1.946$ and $(qR_{g1})^{*(2)} = 3.89$; and (iii) for $52.5 < \chi N_1$, the mixture becomes unstable for two modes, $(qR_{g1,\mathrm{L}})^{(1)} \leq (qR_{g1}) \leq (qR_{g1,\mathrm{R}})^{(1)}$ and $(qR_{g1,\mathrm{L}})^{(2)} \leq (qR_{g1}) \leq (qR_{g1,\mathrm{R}})^{(2)}$. The center of the unstable mode (or the minimum point in $F(q)$) occurring on the left side, $(qR_{g1})_{\mathrm{center}}{}^{(1)}$, shifts toward a smaller q mode with increasing χN_1, whereas the center of the unstable mode occurring on the right side, $(qR_{g1})_{\mathrm{center}}{}^{(2)}$, shifts toward a larger q mode with increasing χN_1.

From Figure 6b, it can be seen that (i) for $\chi N_1 < (\chi N_1)_{\mathrm{s,micro}}{}^{(2)} = 46.6$, the mixture does *not* become *unstable* (i.e., it remains in a stable or metastable state) for microphase transition; (ii) for $\chi N_1 = 46.6$, the mixture becomes unstable for microphase separation at $(qR_{g1})^{*(2)} = 3.89$; (iii) for $46.6 < \chi N_1 < (\chi N_1)_{\mathrm{s,micro}}{}^{(1)} = 112.87$, the q modes near $(qR_{g1})^{*(2)}$, or $(qR_{g1})_{\mathrm{center}}{}^{(2)}$, become unstable; (iv) for $\chi N_1 = 112.87$, the q modes at $(qR_{g1})^{*(1)} = 1.53$ and near $(qR_{g1})^{*(2)}$ become unstable; and (v) for $\chi N_1 > 112.87$, the q modes at both $(qR_{g1})_{\mathrm{center}}{}^{(1)}$ and $(qR_{g1})_{\mathrm{center}}{}^{(2)}$ become unstable, and $(qR_{g1})_{\mathrm{center}}{}^{(1)}$ and $(qR_{g1})_{\mathrm{center}}{}^{(2)}$ shift toward a lower and higher value of q, respectively, with increasing χN_1. Figure 6c can be explained in a similar manner. This system is just complementary to the system considered in Figure 6b. The mode $(qR_{g1})^{*(1)}$ reaches an instability first, and the mode $(qR_{g1})^{*(2)}$ reaches an instability later with increasing χN_1.

Based on Figure 6, plots of $(qR_{g1})^*$ versus ϕ_1 are given in Figure 7a. It can be seen in Figure 7a that (i) $(qR_{g1})^{*(1)}$ is the same (i.e., 1.946) as that for the block copolymer

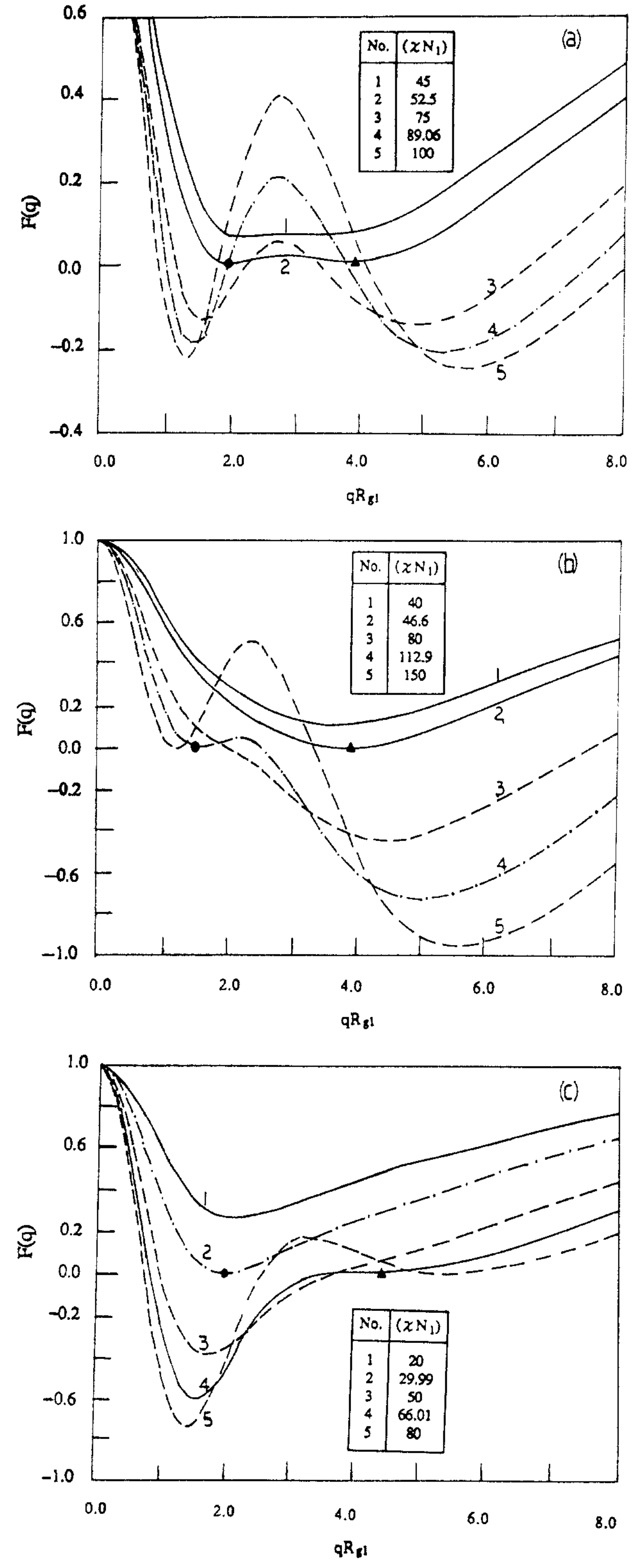

Figure 6. Plots of $F(q)$ versus qR_{g1} for $f_1 = f_3 = 0.5$, $N_3/N_1 = 0.25$, and $\alpha = 0.5$ for various χN_1 at different ϕ_1: (a) $\phi_1 = 0.2$; (b) $\phi_1 = 0.1$; (c) $\phi_1 = 0.35$. Circle and triangle represent microphase separation with $(qR_{g1})^{*(1)}$ and $(qR_{g1})^{*(2)}$, respectively.

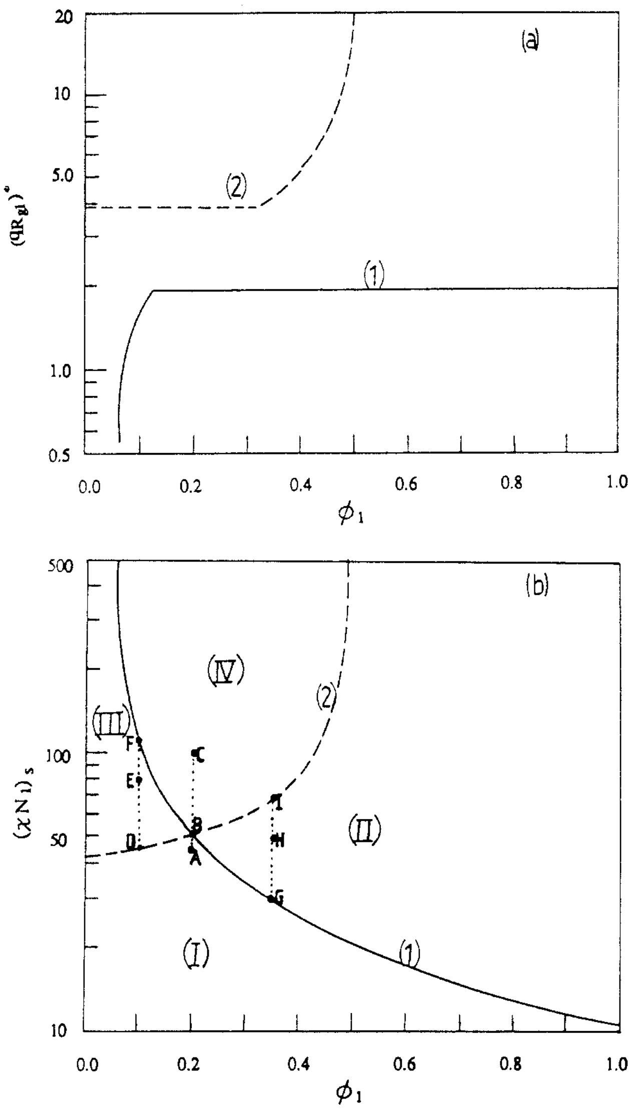

Figure 7. (a) Plots of $(qR_{g1})^{*(1)}$ and $(qR_{g1})^{*(2)}$ versus ϕ_1 for $f_1 = f_3 = 0.5$, $N_3/N_1 = 0.25$, and $\alpha = 0.5$. Curves 1 and 2 represent $(qR_{g1})^{*(1)}$ and $(qR_{g1})^{*(2)}$, respectively. (b) Plots of $(\chi N_1)_s$ versus ϕ_1. Curves 1 and 2 represent $(\chi N_1)_{s,\text{micro}}{}^{(1)}$ and $(\chi N_1)_{s,\text{micro}}{}^{(2)}$, respectively.

(A–B) for $\phi_1 \geq 0.13$ and decreases rapidly with decreasing ϕ_1 and (ii) $(qR_{g1})^{*(2)}$ is the same (i.e., 3.89) as that of the block copolymer (C–D) for $\phi_1 \leq 0.312$ and increases rapidly with increasing ϕ_1. Note that it may be possible that two values of $(qR_{g1})^*$ exist for $\phi_1 < 0.06$ and $\phi_1 > 0.5$ (but not for $\phi_1 = 0$ and 1), although it is very difficult to determine the exact value from numerical computations.

Also based on Figure 6, plots of $(\chi N_1)_s$ versus ϕ_1 are given in Figure 7b. Note that (i) the values of χN_1 at points A–C in Figure 7b were used to generate curves 1, 2, and 5 in Figure 6a, respectively; (ii) the values of χN_1 at points D–F in Figure 7b were used to generate curves 2–4 in Figure 6b, respectively; and (iii) the values of χN_1 at points G–I in Figure 7b were used to generate curves 2–4 in Figure 6c, respectively. It can be seen in Figure 7b that, in the system considered above, there exist four different regimes: (a) regime I, where the mixture does *not* become *unstable* (i.e., it remains in a stable or metastable state) for microphase transition; (b) regime II, where the mixtures become unstable for the q modes near $(qR_{g1})_{\text{center}}{}^{(1)}$, but stable or metastable for the q modes with $(qR_{g1})_{\text{center}}{}^{(2)}$; (c) regime III, where the mixtures become unstable for the q modes near $(qR_{g1})_{\text{center}}{}^{(2)}$, but stable or metastable for the q modes with $(qR_{g1})_{\text{center}}{}^{(1)}$; and (d) regime IV, where the mixtures become unstable for the q modes near $(qR_{g1})_{\text{center}}{}^{(1)}$ and $(qR_{g1})_{\text{center}}{}^{(2)}$. Also note in Figure 7b that (i) $(\chi N_1)_{s,\text{micro}}{}^{(1)}$ corresponding to $(qR_{g1})^{*(1)}$ increases rapidly with decreasing ϕ_1, (ii) $(\chi N_1)_{s,\text{micro}}{}^{(2)}$ corresponding to $(qR_{g1})^{*(2)}$ increases slightly at first and then increases rapidly with increasing ϕ_1, and (iii) these two values become the same at $\phi_1 = 0.2$.

Finally let us consider the spinodal curves and $(qR_{g1})^*$ given in Figure 8 for various values of α for the mixtures considered above (i.e., $f_1 = f_3 = 0.5$ and $N_3 = (^1/_4)N_1$). Note that, for practical purposes, the spinodal points for the

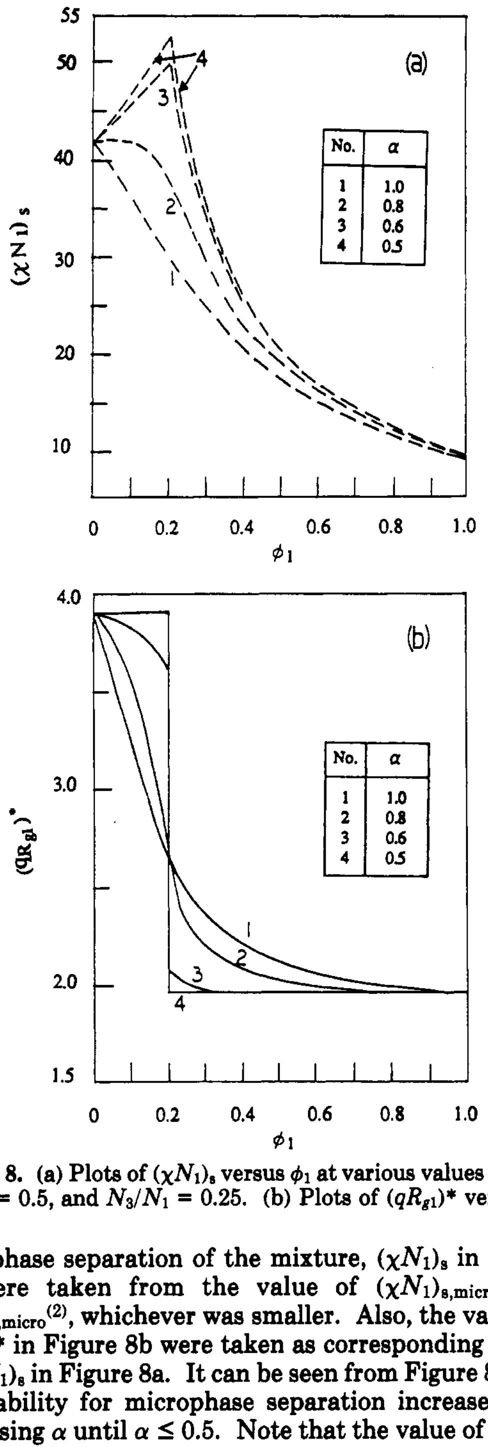

Figure 8. (a) Plots of $(\chi N_1)_s$ versus ϕ_1 at various values of α for $f_1 = f_3 = 0.5$, and $N_3/N_1 = 0.25$. (b) Plots of $(qR_{g1})^*$ versus ϕ_1.

microphase separation of the mixture, $(\chi N_1)_s$ in Figure 8a, were taken from the value of $(\chi N_1)_{s,\mathrm{micro}}{}^{(1)}$ or $(\chi N_1)_{s,\mathrm{micro}}{}^{(2)}$, whichever was smaller. Also, the values of $(qR_{g1})^*$ in Figure 8b were taken as corresponding values of $(\chi N_1)_s$ in Figure 8a. It can be seen from Figure 8a that the stability for microphase separation increases with decreasing α until $\alpha \leq 0.5$. Note that the value of $(\chi N_1)_s$ for $1 - \alpha$ is the same as that for α. For the mixtures considered above, since χ_{eff} obtained from eq 40 becomes zero regardless of the value of α, no macrophase separation will occur. It is of interest to note in Figure 8a that for $\alpha = 0.6$ and 0.5 there exists a discontinuity in $(\chi N_1)_s$ at $\phi_1 = 0.2$ and for $\alpha = 0.8$ there exists a slight maximum near $\phi_1 = 0.07$, which is quite different from the situation having $\alpha = 1$, where $(\chi N_1)_{s,\mathrm{micro}}$ decreases steadily with increasing ϕ_1. Also, at $\phi_1 = 0.2$, $(qR_{g1})^*$ becomes discontinuous for $\alpha = 0.5$ and 0.6, as shown in Figure 8b. These phenomena can be explained by the existence of two values of $(\chi N_1)_{s,\mathrm{micro}}$ which occur at different values of $(qR_{g1})^*$, and these two values are the same at $\phi_1 = 0.2$.

From Figures 6 and 7b, we can conclude that, for specific relationships of R_{ij} such as those given by eq 30, it is possible that two different values of $(\chi N_1)_{s,\mathrm{micro}}$ (i.e., $(\chi N_1)_{s,\mathrm{micro}}{}^{(1)}$ and $(\chi N_1)_{s,\mathrm{micro}}{}^{(2)}$) exist at different values of $(qR_{g1})^*$ (i.e., $(qR_{g1})^{*(1)}$ and $(qR_{g1})^{*(2)}$) and that each value of $(qR_{g1})^*$ varies with ϕ_1. These results can be tested experimentally using small-angle X-ray scattering by choosing a mixture of two block copolymers. It should be mentioned that even for the (A–B)$_1$/(A–B)$_2$ mixture, where $f_1 = f_3 = 0.5$ and $N_3 \ll N_1$, it may be possible that two spinodal points exist for the microphase separation at different values of q^*.[18] But, $(qR_{g1})^{*(1)}$ and $(qR_{g1})^{*(2)}$ do not vary with ϕ_1, which is different from the situation of the (A–B)/(C–D) mixture, where these two values change with ϕ_1, as shown in Figure 7a. Note further that for the (A–B)$_1$/(A–B)$_2$ mixture where $f_1 = f_3 = 0.5$ and N_3 is not much different from N_1 (e.g., $N_3/N_1 = {}^1/_4$), there exists only one value of the spinodal for the microphase separation.

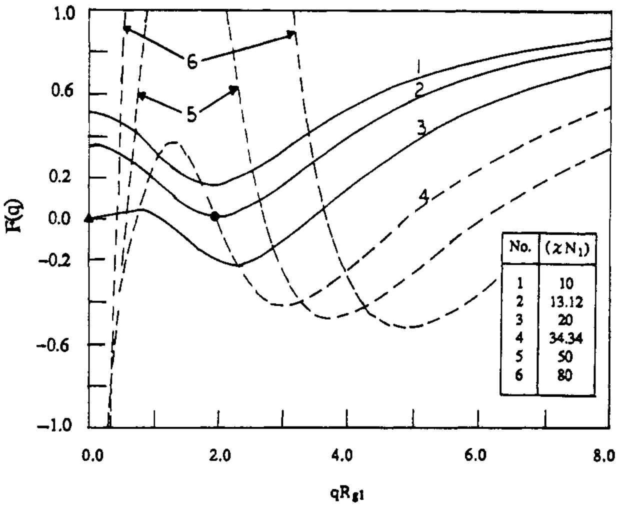

Figure 9. Plots of $F(q)$ versus qR_{g1} for $f_1 = 0.5$, $N_3 = N_4 = ({}^1/_2)N_1$, $\phi_3 = \phi_4 = ({}^1/_2)\phi_1$, $\phi_1 = 0.8$, and $\alpha = 0.5$ for various χN_1. Circle and triangle represent microphase and macrophase separations, respectively.

(c) Mixture of Block Copolymer (A–B) and Two Homopolymers C and D. For mixtures of block copolymer (A–B) and two homopolymers C and D, $S_{ij}(q)$ are given by

$$S_{11}(q) = \phi_1 N_1 g(f_1, N_1) \quad (43a)$$

$$S_{22}(q) = \phi_1 N_1 g(1-f_1, N_1) \quad (43b)$$

$$S_{33}(q) = \phi_3 N_3 g(1, N_3) \quad (43c)$$

$$S_{44}(q) = \phi_4 N_4 g(1, N_4) \quad (43d)$$

$$S_{12}(q) = ({}^1/_2)\phi_1 N_1 [g(1, N_1) - g(f_1, N_1) - g(1-f_1, N_1)] \quad (43e)$$

$$S_{13}(q) = S_{14}(q) = S_{23}(q) = S_{24}(q) = S_{34}(q) = 0 \quad (43f)$$

where ϕ_1, ϕ_3, and ϕ_4 are the volume fractions of (A–B), C, and D, respectively; N_1, N_3, and N_4 are the degrees of polymerization (or numbers of statistical segments) for (A–B), C, and D; and f_1 is the volume fraction of component A in block polymer (A–B).

Let us again consider a special case where the interaction parameters are given by eq 30. For $f_1 = 0.5$, $N_3 = N_4 = ({}^1/_2)N_1$, $\phi_3 = \phi_4 = (1 - \phi_1)/2$, and $\alpha = 0.5$, plots of $F(q)$ versus qR_{g1} for various values of χN_1 at $\phi_1 = 0.8$ are given in Figure 9. It can be seen in Figure 9 that (i) for $\chi N_1 < (\chi N_1)_{s,\mathrm{micro}} = 13.12$, the mixture does *not* become *unstable* (i.e., it remains in a stable or metastable state) for both microphase and macrophase separations; (ii) for $\chi N_1 = 13.12$, $F(q^*)$ is zero at $(qR_{g1})^* = 1.946$, which corresponds to the spinodal for microphase separation, and the q mode satisfying $(qR_{g1})^* = 1.946$ becomes unstable; (iii) for $\chi N_1 = (\chi N_1)_{s,\mathrm{macro}} = 20$, $F(q^*{=}0)$ is equal to zero, which corresponds to the spinodal for macrophase transition where the q modes satisfying both 0 and $1.06 \leq qR_{g1} \leq 3.47$ become unstable; (iv) for $\chi N_1 > 20$ (e.g., $\chi N_1 = 50$), the

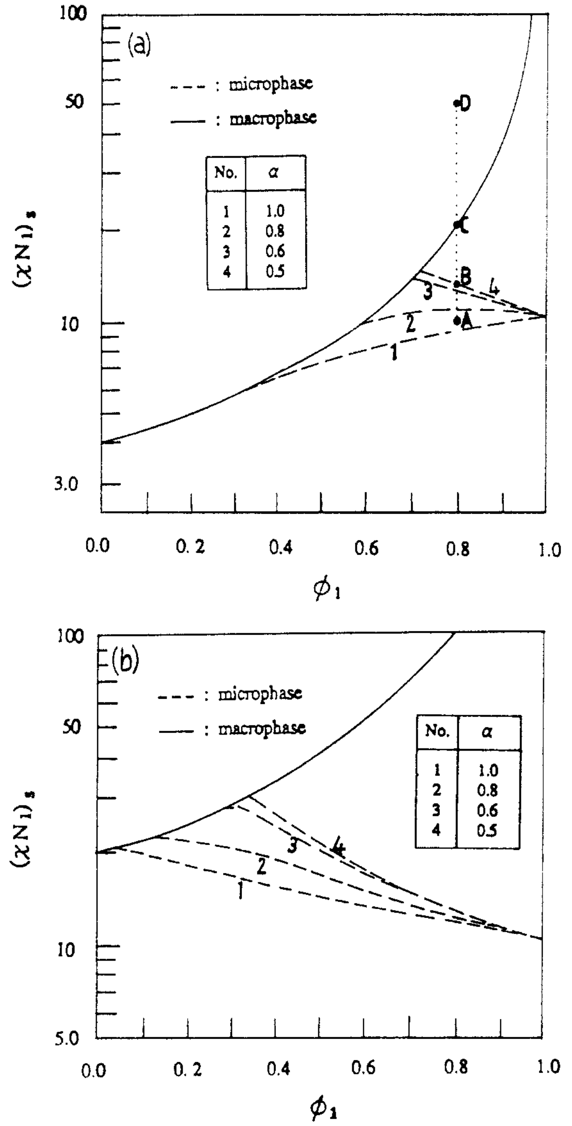

Figure 10. Plots of $(\chi N_1)_s$ versus ϕ_1 for $f_1 = 0.5$, $N_3 = N_4$, and $\phi_3 = \phi_4 = (^1/_2)\phi_1$ at various values of α for different ratios of N_3/N_1: (a) 0.5; (b) 0.1.

q modes satisfying $0 \leq qR_{g1} \leq 0.58$ and $2.71 \leq qR_{g1} \leq 6.06$ become unstable; and (v) $(qR_{g1})_{\mathrm{center}}$, which is a minimum point in the second unstable region of microphase transition appearing in curves 4–6, shifts toward a larger value of q with increasing χN_1. It should be noted that curves 5 and 6 in Figure 9 are very similar to curves 5 and 6 in Figure 1a. Therefore, for larger values of χN_1, the unstable region appearing on the left side is related to macrophase separation, whereas the unstable region on the right side is related to microphase transition.

Based on Figure 9, plots of $(\chi N_1)_s$ versus ϕ_1 are given in Figure 10a for various values of α $(0.5 \leq \alpha \leq 1)$. Note that the values of χN_1 at points A–D in Figure 10a were used to generate curves 1–3 and 5 in Figure 9, respectively. Also, plots of χN_1 versus ϕ_1 for $N_3/N_1 = 0.1$, $f_1 = 0.5$, and $\phi_3 = \phi_4 = (^1/_2)(1 - \phi_1)$ are given in Figure 10b. It can be seen in Figure 10a that (i) for $\alpha = 1$ (i.e., the mixture of the block copolymer $(\mathrm{A{-}B})_1$ and two homopolymers A and B), both $(\chi N_1)_{s,\mathrm{micro}}$ and $(\chi N_1)_{s,\mathrm{macro}}$ decreases with decreasing ϕ_1; (ii) for $\alpha = 0.8$, $(\chi N_1)_{s,\mathrm{micro}}$ initially increases and then decreases with decreasing ϕ_1; (iii) for $\alpha = 0.6$ and 0.5, $(\chi N_1)_{s,\mathrm{micro}}$ increases rapidly with decreasing ϕ_1; and (iv) $(\chi N_1)_{s,\mathrm{macro}}$ is independent of α at a given ϕ_1. Note that both $(\chi N_1)_{s,\mathrm{micro}}$ and $(\chi N_1)_{s,\mathrm{macro}}$ for $1 - \alpha$ are the same as those for α. It should be mentioned that curve 1 in Figure 10a (i.e., $\alpha = 1$ or 0) was reported previously.[42]

The spinodal curves for the macrophase separation in Figure 10a were obtained by substituting eqs 19, 20, and 43 into eq 38:

$$1/(N_1\phi_1N_3\phi_3) + 1/(N_3\phi_3N_4\phi_4) + 1/(N_1\phi_1N_4\phi_4) - 2(\chi_{13}'/N_4\phi_4 + \chi_{14}'/N_3\phi_3 + \chi_{34}/N_1\phi_1) + 2(\chi_{13}'\chi_{34} + \chi_{34}\chi_{14}' + \chi_{13}'\chi_{14}') - [(\chi_{13}')^2 + (\chi_{14}')^2 + (\chi_{34})^2] = 0 \quad (44)$$

where

$$\chi_{13}' = f_1\chi_{13} + (1 - f_1)\chi_{23} - f_1(1 - f_1)\chi_{12} \quad (45a)$$

$$\chi_{14}' = f_1\chi_{14} + (1 - f_1)\chi_{24} - f_1(1 - f_1)\chi_{12} \quad (45b)$$

Note that eq 44 can also be obtained from eq 48 in ref 20.

For $f_1 = 0.5$, $N_3 = N_4 = \gamma N_1$, and $\phi_3 = \phi_4 = (1 - \phi_1)/2$, which is the same situation considered in Figure 10, eq 44 reduces to

$$(\chi N_1)_{s,\mathrm{macro}} = 2/[\gamma(1 - \phi_1)] \quad (46)$$

From eq 46 we observe that $(\chi N_1)_{s,\mathrm{macro}}$ decreases with decreasing ϕ_1 and $(\chi N_1)_{s,\mathrm{macro}}$ is independent of α at a given ϕ_1 (see Figure 10).

It should be mentioned that both $(\chi N_1)_{s,\mathrm{micro}}$ and the region of the spinodal for macrophase transition (i.e., $\phi_{1,\mathrm{CR}}$) increase with decreasing α until α reaches 0.5 for mixtures of block copolymer (A–B) and two homopolymers C and D, as shown in Figure 10. On the other hand, the region of the spinodal for macrophase transition $(\phi_{1,\mathrm{CR}} - \phi_{1,\mathrm{CL}})$ decreases, whereas $(\chi N_1)_{s,\mathrm{micro}}$ increases with increasing α for mixtures of two block copolymers, (A–B) and (C–D), as shown in Figure 4a–d.

When the ratio $N_3/N_1 = N_4/N_1$ is decreased to 0.1, the microphase transition region is greatly extended, as shown in Figure 10b, although the general trend is similar to that in Figure 10a.

IV. Concluding Remarks

In this paper, we have presented a new method for calculating the structure factors $\tilde{S}_{ij}(q)$ for multicomponent polymer systems using the random-phase approximation and incompressibility constraint. Specifically, we have derived eq 12 for an m-component polymer system and obtained $\tilde{S}_{ij}(q)$ in explicit form given in eqs 17–21 for 4-component polymer systems. We then considered, for illustration purposes, spinodal curves (or stability limits) for two 4-component polymer systems, namely (i) mixtures of two block copolymers, (A–B)/(C–D), and (ii) mixtures of a block copolymer, (A–B), and two homopolymers, C and D. We have found that under certain relationships between the χ_{ij}, in the mixtures of two block copolymers (A–B) and (C–D) having different chemical structures, two spinodal transitions for microphase separation are possible at two different values of $(qR_{g1})^*$ and that each $(qR_{g1})^*$ changes with ϕ_1. Note that, in the most general situation, we need six Flory interaction parameters, χ_{ij}, for the 4-component polymer systems considered above. The predictions made in this study must await the results of careful experimental investigation in the future.

In deriving eq 12, we have imposed the incompressibility constraint. Recently, Freed and co-workers[31–35] raised questions about the validity of the incompressibility constraint for block copolymer melts. At present, however, there is not sufficient experimental evidence, which either supports or rejects the validity of the incompressibility constraint, that has been used in the derivation of various expressions for the structure factors for block copolymers using the RPA method.[7,8,11–24] We must await the results of careful experiment, which will enable us to determine the validity of (or reject) the incompressiblity constraint often used in RPA calculations.

Acknowledgment. J.K.K. thanks Dr. J. K. Yeo, Managing Director of the R & D center, Lucky Ltd., for his encouragement during this work. We thank Professor C. D. Han for helpful discussion and a critical reading of the manuscript.

Appendix I

For the mixtures of a block copolymer (A–B) and a homopolymer C, we have

$$\delta\mathbf{S}_o(q) = 0 \tag{A1}$$

and, $\mathbf{S}_o^{-1}(q)\cdot(\mathbf{X} + \mathrm{v}_o\xi_o)$ is given by

$$\begin{bmatrix} -\chi_{13} + 1/S_{33}(\mathrm{q}) & -\chi_{23} + 1/S_{33}(\mathrm{q}) \\ -\chi_{13} + 1/S_{33}(\mathrm{q}) & -\chi_{23} + 1/S_{33}(\mathrm{q}) \end{bmatrix} \tag{A2}$$

Also, from eqs 16b, A1, and A2 we have

$$\mathbf{U}(q) = \begin{bmatrix} -2\chi_{13} + 1/S_{33}(\mathrm{q}) & \chi_{12} - \chi_{13} - \chi_{23} + 1/S_{33}(\mathrm{q}) \\ \chi_{12} - \chi_{13} - \chi_{23} + 1/S_{33}(\mathrm{q}) & -2\chi_{23} + 1/S_{33}(\mathrm{q}) \end{bmatrix} \tag{A3}$$

Note that $\mathbf{U}_{11}(q)$ (or $\mathbf{U}_{22}(q)$) in eq A3 is the same as eq 19a in ref 15 and $\mathbf{U}_{12}(q)$ in eq A3 is the same as eq 19b in ref 15. In order to calculate $\tilde{S}_{ij}(q)$, we first consider $\tilde{\mathbf{S}}^{-1}(q)$. From eqs 14 and A2, we have

$$\tilde{S}^{-1}(q) = \begin{bmatrix} S_{22}(q)/d + U_{11}(q) & -S_{12}(q)/d + U_{12}(q) \\ -S_{12}(q)/d + U_{12}(q) & S_{11}(q)/d + U_{22}(q) \end{bmatrix} \tag{A4}$$

where $U_{ij}(q)$ are given by eq A3 and d is given by

$$d = S_{11}(q)S_{22}(q) - [S_{12}(q)]^2 \tag{A5}$$

The inversion of matrix $\tilde{\mathbf{S}}^{-1}(q)$ is given by[16]

$$\mathbf{S}(q) = \frac{1}{\Delta}\begin{bmatrix} S_{11}(q) + U_{22}(q)d & S_{12}(q) - U_{12}(q)d \\ S_{12}(q) - U_{12}(q)d & S_{22}(q) + U_{11}(q)d \end{bmatrix} \tag{A6}$$

where Δ is given by

$$\Delta = 1 + S_{11}(q)U_{11}(q) + S_{22}(q)U_{22}(q) + 2S_{12}(q)U_{12}(q) + d[U_{11}(q)U_{22}(q) - U_{12}^2(q)] \tag{A7}$$

Note that $\tilde{S}_{11}(q)$ (or $\tilde{S}_{22}(q)$) in eq A6 is the same as eq 9a in ref 16 and $\tilde{S}_{12}(q)$ in eq A6 is the same as eq 9b in ref 16.

Let us now consider the 4-component polymer systems for which each component of $\mathbf{U}(q)$ is known and $\delta\mathbf{S}_o(q)$ is a zero matrix. In this situation, $\tilde{S}_{ij}^{-1}(q)$ is easily calculated from eq 13:

$$\tilde{S}_{ij}^{-1}(q) = S_{oij}^{-1}(q) + U_{ij}(q) \tag{A8}$$

On the other hand, the calculation of $\tilde{S}_{ij}(q)$ from $\tilde{S}_{ij}^{-1}(q)$ requires the solution of six nonlinear equations:

$$[\tilde{S}_{11}(q)\tilde{S}_{22}(q) - \tilde{S}_{12}^2(q)]/\tilde{D} = [S_{11}(q)S_{22}(q) - S_{12}^2(q)]/D + U_{33}(q) \tag{A9a}$$

$$[\tilde{S}_{11}(q)\tilde{S}_{33}(q) - \tilde{S}_{13}^2(q)]/\tilde{D} = [S_{11}(q)S_{33}(q) - S_{13}^2(q)]/D + U_{22}(q) \tag{A9b}$$

$$[\tilde{S}_{22}(q)\tilde{S}_{33}(q) - \tilde{S}_{23}^2(q)]/\tilde{D} = [S_{22}(q)S_{33}(q) - S_{23}^2(q)]/D + U_{11}(q) \tag{A9c}$$

$$[\tilde{S}_{23}(q)\tilde{S}_{13}(q) - \tilde{S}_{12}(q)\tilde{S}_{33}(q)]/\tilde{D} = [S_{23}(q)S_{13}(q) - S_{12}(q)S_{33}(q)]/D + U_{12}(q) \tag{A9d}$$

$$[\tilde{S}_{12}(q)\tilde{S}_{23}(q) - \tilde{S}_{22}(q)\tilde{S}_{13}(q)]/\tilde{D} = [S_{12}(q)S_{23}(q) - S_{22}(q)S_{13}(q)]/D + U_{13}(q) \tag{A9e}$$

$$[\tilde{S}_{12}(q)\tilde{S}_{13}(q) - \tilde{S}_{11}(q)\tilde{S}_{23}(q)]/\tilde{D} = [S_{12}(q)S_{13}(q) - S_{11}(q)S_{23}(q)]/D + U_{23}(q) \tag{A9f}$$

where

$$\tilde{D} = \tilde{S}_{11}(q)[\tilde{S}_{22}(q)\tilde{S}_{33}(q) - \tilde{S}_{23}^2(q)] - \tilde{S}_{12}(q)[\tilde{S}_{12}(q)\tilde{S}_{33}(q) - \tilde{S}_{13}(q)\tilde{S}_{23}(q)] + \tilde{S}_{13}(q)[\tilde{S}_{12}(q)\tilde{S}_{23}(q) - \tilde{S}_{13}(q)\tilde{S}_{22}(q)] \tag{A10a}$$

$$D = S_{11}(q)[S_{22}(q)S_{33}(q) - S_{23}^2(q)] - S_{12}(q)[S_{12}(q)S_{33}(q) - S_{13}(q)S_{23}(q)] + S_{13}(q)[S_{12}(q)S_{23}(q) - S_{13}(q)S_{22}(q)] \tag{A10b}$$

Note that the solution of eqs A9 and A10 for $\tilde{S}_{ij}(q)$ requires an initial guess for each value of $\tilde{S}_{ij}(q)$ $(i,j = 1, 2, 3)$, which is rather difficult. Without having a reasonable approximation for each $\tilde{S}_{ij}(q)$, the solution of eqs A9 and A10 is difficult to obtain.

Appendix II

From ref 8, the spinodal point can be obtained from

$$a(q^*)c(q^*) = [b(q^*)]^2 \tag{B1}$$

Substitution of eqs 2.21–2.23 in ref 8 into eq B1, after some rearrangement, gives (see eq B4 in ref 43)

$$[(1 - a_o - b_o) - 4a_ob_o](\chi r_c\phi_c)^2 + 2\{[a_og_{AA}(q) + b_og_{BB}(q) - (1 - a_o - b_o)g_{AB}(q)]/D_2(q) + 1/A(q)\}(\chi r_c\phi_c) - [1 + S_2(q)/A(q)]/D_2(q) = 0 \tag{B2}$$

where

$$D_2(q) = g_{AA}(q)g_{BB}(q) - [g_{AB}(q)]^2 \tag{B3a}$$

$$S_2(q) = g_{AA}(q) + g_{BB}(q) + 2g_{AB}(q) \tag{B3b}$$

$$A(q) = \phi_H r_H g_H(q)/\phi_c r_c$$

$$a_o = \chi_{AH}/\chi \qquad b_o = \chi_{BH}/\chi \tag{B3c}$$

Also, the spinodal point is given by

$$F(q^*) = 0 \tag{B4}$$

From eq 19 for $m = 3$ and eq B4, we have

$$-F(q^*)[S_3(q)/W_3(q)] = (\chi_{12}^2 + \chi_{13}^2 + \chi_{23}^2) - 2(\chi_{12}\chi_{13} + \chi_{12}\chi_{23} + \chi_{13}\chi_{23}) - [S_3(q)/W_3(q)]\{1 + 2[\bar{S}_{12}(q)\chi_{12} + \bar{S}_{13}(q)\chi_{13} + \bar{S}_{23}(q)\chi_{23}]\} = 0 \tag{B5}$$

where

$$S_{11}(q) = \phi_C r_C g_{AA}(q) \qquad S_{12}(q) = \phi_C r_C g_{AB}(q)$$
$$S_{22}(q) = \phi_C r_C g_{BB}(q) \tag{B6a}$$

$$S_{33}(q) = \phi_H r_H g_H(q) \qquad S_{13}(q) = S_{23}(q) = 0 \tag{B6b}$$

$$S_3(q) = S_{11}(q) + S_{22}(q) + S_{33}(q) + 2S_{12}(q) \tag{B6c}$$

$$W_3(q) = [S_{11}(q)S_{22}(q) - S_{12}(q)^2]S_{33}(q) \tag{B6d}$$

Note that in deriving eq B5 from eq 19, the following relationships are used:

$$W_4(q) = 0 \qquad S_4(q) = S_3(q) \tag{B7a}$$

$$D_{2,1212}(q) = D_{2,1313}(q) = D_{2,2323}(q) = -(^1/_4)W_3(q)/S_3(q) \tag{B7b}$$

$$D_{2,1213}(q) = D_{2,1223}(q) = D_{2,1323}(q) = (^1/_4)W_3(q)/S_3(q) \tag{B7c}$$

From eqs B6 and B3 we have

$$S_3(q)/W_3(q) = [1 + S_2(q)/A(q)]/[D_2(q)(\phi_C r_C)^2] \tag{B8}$$

Also, we have

$$[S_3(q)/W_3(q)][\bar{S}_{12}(q) + b_o\bar{S}_{23}(q) + a_o\bar{S}_{13}(q)] = \{[-a_o g_{AA}(q) - b_o g_{BB}(q) + (1 - a_o - b_o)g_{AB}(q)]/D_2(q) - 1/A(q)\}/(\phi_C r_C) \tag{B9}$$

Finally, substitution of eqs B8 and B9 into eq B5, after some rearrangements, yields eq B2.

References and Notes

(1) Utracki, L. A. *Polymer Alloys and Blends*; Oxford University Press: New York, 1989.
(2) Noolandi, J.; Hong, K. M. *Macromolecules* **1982**, *15*, 382; **1984**, *17*, 1531.
(3) Noolandi, J. *Polym. Eng. Sci.* **1984**, *24*, 70.
(4) Vilgis, T. A.; Noolandi, J. *Macromolecules* **1990**, *23*, 2341.
(5) Leibler, L. *Makromol. Chem. Macromol. Symp.* **1988**, *16*, 1.
(6) Shull, K. K.; Kramer, E. J. *Macromolecules* **1990**, *23*, 4769.
(7) Hong, K. M.; Noolandi, J. *Macromolecules* **1983**, *16*, 1083.
(8) Whitmore, M. D.; Noolandi, J. *Macromolecules* **1985**, *18*, 2486.
(9) de Gennes, P. G. *J. Phys. (Paris)* **1970**, *31*, 235.
(10) de Gennes, P. G. *Scaling Concepts in Polymer Physics*; Cornell University Press: New York, 1979.
(11) Leibler, L. *Macromolecules* **1980**, *13*, 1602.
(12) Leibler, L.; Benoit, H. *Polymer* **1981**, *22*, 195.
(13) Benoit, H.; Wu, W.; Benmouna, M.; Mozer, B.; Bauer, B.; Lapp, A. *Macromolecules* **1985**, *18*, 986.
(14) Benoit, H.; Benmouna, M.; Wu, W. *Macromolecules* **1990**, *23*, 1511.
(15) Vilgis, T.; Benmouna, M.; Benoit, H. *Macromolecules* **1991**, *24*, 4481.
(16) Benmouna, M.; Vilgis, T. *Macromolecules* **1991**, *24*, 3866.
(17) de la Cruz, M. O.; Sanchez, I. C. *Macromolecules* **1986**, *19*, 2501.
(18) Mori, K.; Tanaka, H.; Hashimoto, T. *Macromolecules* **1987**, *20*, 381.
(19) Nojima, S.; Roe, R. J. *Macromolecules* **1987**, *20*, 1866.
(20) Ijichi, Y.; Hashimoto, T. *Polym. Commun.* **1988**, *29*, 135.
(21) Hashimoto, T.; Ijichi, Y.; Fetters, L. J. *J. Chem. Phys.* **1988**, *89*, 2463.
(22) Ijichi, Y.; Hashimoto, T.; Fetters, L. J. *Macromolecules* **1989**, *22*, 2817.
(23) Benoit, H.; Hadziioannou, G. *Macromolecules* **1988**, *21*, 1449.
(24) Mori, K.; Tanaka, H.; Hasegawa, H.; Hashimoto, T. *Polymer* **1989**, *30*, 1389.
(25) (a) Tanaka, H.; Sakurai, S.; Hashimoto, T.; Whitmore, M. D. *Polymer* **1992**, *33*, 1006. (b) Tanaka, H.; Hashimoto, T. *Macromolecules* **1991**, *24*, 5398. (c) Sakurai, S.; Mori, K.; Okawara, A.; Kimishima, K.; Hashimoto, T. *Macromolecules* **1992**, *25*, 2679.
(26) Bates, F. S.; Hartney, M. A. *Macromolecules* **1985**, *18*, 2478; **1986**, *19*, 2892.
(27) Hong, K. M.; Noolandi, J. *Polym. Commun.* **1984**, *25*, 265.
(28) Berger, C.; Ruland, W.; Semenov, A. N. *Macromolecules* **1990**, *23*, 3339; **1991**, *24*, 816.
(29) Brereton, M. G.; Vilgis, T. A. *J. Phys. (Paris)* **1899**, *50*, 245.
(30) Benoit, H. *Polymer* **1991**, *32*, 579.
(31) McMullen, W. E.; Freed, K. F. *Macromolecules* **1990**, *23*, 255.
(32) Dudowicz, J.; Freed, K. F. *Macromolecules* **1990**, *23*, 1519.
(33) Tang, H.; Freed, K. F. *Macromolecules* **1991**, *24*, 958.
(34) Dudowicz, J.; Freed, K. F. *Macromolecules* **1991**, *24*, 5112.
(35) Dudowicz, J.; Freed, K. F. *J. Chem. Phys.* **1992**, *96*, 9147.
(36) Sanchez, I. C.; Lacomb, R. H. *Macromolecules* **1978**, *11*, 1145.
(37) $2[W_3(q)/S(q)](\chi_{12} - \chi_{13} - \chi_{23})$ in eq 15 of ref 20 should read as $[W_3(q)/S_3(q)](\chi_{12} - \chi_{13} - \chi_{23})$.
(38) There exist two minima in $F(q)$ at $q = 0$ and $qR_{g1} = (qR_{g1})_{\text{center}} \neq 0$ in curves 5 and 6 in Figure 1a, although values of $F(q)$ near $q = 0$ are not displayed.
(39) Kambour, R. P.; Bendler, J. T.; Bopp, R. C. *Macromolecules* **1983**, *16*, 753.
(40) Ten Brinke, G.; Karasz, F. E.; MacKnight, W. J. *Macromolecules* **1983**, *16*, 1827.
(41) Paul, D. J.; Barlow, J. W. *Polymer* **1984**, *25*, 487.
(42) Tanaka, H.; Hashimoto, T. *Polym. Commun.* **1988**, *29*, 212.
(43) Han, C. D.; Kim, J.; Kim, J. K.; Chu, S. G. *Macromolecules* **1989**, *22*, 3443.